Submitted to International Journal of Fatigue
Virtual Special Issue: Multiaxial Fatigue 2019
October 2019
REVISED Version R1, November 2019

MEAN STRESS EFFECT ON FATIGUE LIFE ESTIMATION FOR INCONEL 718 ALLOY

Sabrina Vantadori*, Andrea Carpinteri*, Raimondo Luciano**,
Camilla Ronchei***, Daniela Scorza**, Andrea Zanichelli*

*Department of Engineering & Architecture, University of Parma,
Parco Area delle Scienze 181/A, 43124 Parma, Italy

** Department of Engineering, University of Naples Parthenope,
Centro Direzionale Isola C4, 80143 Naples, Italy

*** Department of Civil Engineering, University of Calabria,
via Pietro Bucci, 87036 Arcavacata di Rende (CS), Italy

Corresponding author: sabrina.vantadori@unipr.it

ABSTRACT

Uniaxial and biaxial fatigue tests related to Inconel 718 specimens are analysed using the critical plane-based multiaxial fatigue criterion by Carpinteri et al. in conjunction with a Smith-Watson-Topper (SWT) type of relationship. More precisely, specimens subjected to proportional and non-proportional loading under strain control are examined, such loadings being characterised by both zero and non-zero mean values. Fatigue life is computed through the novel formulation proposed here and compared with the experimental fatigue life in terms of number of loading cycles needed to form a surface crack whose length is equal to 1 mm.

KEYWORDS: critical plane, fatigue life, strain-based criterion, SWT

NOMENCLATURE

1, 2, 3	principal strain directions
b	strength exponent
c	ductility exponent
C_a	shear stress amplitude related to the critical plane
E	Young's modulus
N_{exp}	experimental fatigue life
N_f	fatigue life
$N_{\max}$	maximum normal stress related to the critical plane
P	material point
$P\hat{1}\hat{2}\hat{3}$	averaged principal strain frame
$Puvw$	local reference system attached to the critical plane
$Prtz$	fixed reference system
T	period
T_{RMS}	mean square error
t	time
$\mathbf{w}$	unit vector normal to the critical plane
γ_{zt}	shear strain
β	phase shift
$\boldsymbol{\varepsilon}$	strain tensor at point P
$\varepsilon_1, \varepsilon_2, \varepsilon_3$	principal strains
ε'_f	ductility coefficient
ε_a	applied normal strain amplitude
$\varepsilon_{eq,a}$	equivalent normal strain amplitude
ε_z	axial normal strain
$\boldsymbol{\eta}$	displacement vector at verification point P, related to the critical plane

$\boldsymbol{\eta}_N$	normal vector component of $\boldsymbol{\eta}$, related to the critical plane
$\boldsymbol{\eta}_C$	tangential vector component of $\boldsymbol{\eta}$, related to the critical plane
ν_{eff}	effective Poisson's ratio
σ'_f	strength coefficient
$\sigma_{af,-1}$	fully-reversed normal stress fatigue strength
$\sigma_{eq,\max}$	maximum value of the equivalent normal stress
$\sigma_{\max}$	maximum value of the measured normal stress
σ_z	axial normal stress
$\tau_{af,-1}$	fully-reversed shear stress fatigue strength
τ_{zt}	shear stress
ϕ, θ, ψ	principal Euler angles

Subscripts

a	amplitude
m	mean value
max	maximum value

1. INTRODUCTION

As is well-known, the regime of fatigue loading (low-cycle or high-cycle fatigue), the controlled variable of experimental testing, and the grade of material ductility significantly influence the uniaxial fatigue cracking behaviour of metals **[1]**.

At high stress-intensity factor range value, typical of low-cycle fatigue (LCF) testing, crack growth predominantly occurs on planes of maximum shear loading. This mechanism was termed Stage I by Forsyth **[2]**. Being such a testing generally performed on ductile materials (since the plastic zone surrounding the crack tip can encompass many grains), the Stage I mechanism may be even associated to ductile materials. Such a statement can be found in Ref.**[3]** by Macha, where Stage I is supposed to dominate in ductile materials.

At low stress-intensity factor range value, typical of high-cycle fatigue (HCF) testing, crack growth predominantly occurs on the plane oriented perpendicular to the maximum principal loading direction. This mechanism was termed Stage II by Forsyth **[2]**. Being such a testing generally performed on brittle and extremely brittle materials (since the plastic zone surrounding the crack tip is confined to only a few grains), the Stage II mechanism may be even associated to brittle and extremely brittle materials. Such a statement can be found in Ref.**[3]** by Macha, where Stage II is supposed to dominate in brittle materials.

These mechanisms are schematically represented in **Figure 1**, where the ratio between the number N of loading cycles and the

fatigue life N_f is plotted against N_f, similar to that reported in Ref. **[1]**. **Figure 1(a)** shows the transition between (i) crack nucleation, (ii) Stage I and (iii) Stage II crack growth for a ductile material under LCF regime, that shows a high number of loading cycles spent to propagate the crack under Stage I. On the other hand, the above transition under HCF for extremely brittle and brittle materials, respectively, is represented in **Figures 1(b)** and **(c)**. More precisely, for extremely brittle materials under HCF regime, only Stage II crack propagation occurs (**Figure 1(b)**), whereas both Stage I and Stage II propagation occur for brittle materials (**Figure 1(c)**). Note that **Figure 1(b)** graphically represents the statement in Ref.**[4]** by Brown, where Stage I cracking is observed to play a significant role in long life or high-cycle fatigue (see the nucleation region in **Figure 1(b)**).

Note that the shape of each curve in **Figure 1** depends on both material and loading type **[1]**.

Figure 1.

The above transition is experimentally observed even in multiaxial fatigue **[5,6]**.

Since multiaxial experiments are expensive, and even may not be able to simulate the actual loading conditions, many multiaxial criteria for metallic alloys have been proposed in the literature to address fatigue failure and corresponding fatigue life.

By focusing the attention on multiaxial LCF, several total life approaches have been proposed in the literature and, among them, criteria based on strain components or energy, both related to the so-called critical plane **[7-9].** Note that, under such a fatigue regime, both strain tensor components and energy can be easily computed since tests are generally performed under strain control (that is, the strain is the controlled variable) and stress-strain loop data are registered during tests (that is, the uncontrolled variable is registered, too). A review of the first criteria proposed in the literature in such a context may be found in Ref.**[3].**

It is important to highlight that, under strain-controlled uniaxial and multiaxial fatigue testing, mean stress effect has to be taken into account in the criteria formulation. In particular, for uniaxial fatigue loading, several models are available in the literature in order to take into account the above mean stress effect **[10,11].**

This issue is more complex in the case of multiaxial fatigue loading. In such a context, a novel formulation is proposed in the present paper employing the critical plane-based criterion by Carpinteri et al. formulated in terms of strains **[12]** together with a relationship similar to that by Smith-Watson-Topper (SWT) **[13].**

Note that, although the novel formulation can be employed to simulate experimental tests under any fatigue regime, it has two limitations in LCF regime. More precisely, it can be used when:

(a) the metal is brittle/extremely brittle or the metal behaviour is between brittle and ductile because, when the metal is ductile, the effect of loading non-proportionality is not implemented in such a formulation;

(b) the tests to be simulated have to be under strain-control or stress-control with zero mean values, because the ratcheting phenomenon observed under stress-control with mean values different from zero is not implemented in such a formulation.

Note that many Authors **[14-17]** use the ratio $\tau_{af,-1}/\sigma_{af,-1}$ (between pure torsion and pure tension fatigue strength at a given number of loading cycles) as an indicator of ductility **[18]**, in order to define if the material behaviour is ductile, brittle, or extremely brittle. They suggest that ductile materials have a ratio $\tau_{af,-1}/\sigma_{af,-1} \leq 1/\sqrt{3}$, extremely brittle materials have a ratio close to 1, whereas for brittle materials the ratio ranges between $1/\sqrt{3}$ and 1, as was experimentally proved by Gough **[14]** and Fukuda et al. **[16]**.

Summarizing, the first limitation consists in the exclusion of the very ductile metal simulation under LCF non-proportional loading. As a matter of fact, it was experimentally observed that, when the metal is brittle/extremely brittle, the effect of loading non-proportionality is negligible on fatigue life, whereas the opposite occurs for a ductile metal, as was reported in Ref.**[19]**.

The second limitation consists in the exclusion of the LCF test simulation under stress-control with mean values different from zero, but that does not seem so crucial due to the fact that LCF tests are generally performed under strain-control.

The effectiveness of the proposed formulation is hereafter evaluated by means of some strain-controlled fatigue test data **[20-22]**. Such data are related to tension, torsion and combined tension-torsion fatigue tests (with zero and non-zero mean values) carried out on specimens made of Inconel 718 alloy. More precisely, the theoretical results computed through the novel formulation are compared with the experimental ones in terms of number of loading cycles to failure, here defined as the number of loading cycles needed to form a surface crack with length equal to 1 mm.

The paper is structured as follows: Section 2 briefly reviews the mean stress effect on fatigue life. In Section 3, the theoretical basics of the Carpinteri et al. criterion formulated in terms of strains **[12]** are outlined, by also implementing a like SWT relationship. Section 4 summarises the experimental campaign reported in Refs **[20-22]** as far as material mechanical properties, specimen geometry, testing procedure, and presents the experimental results. Such data are used to validate the novel formulation, as is discussed in Section 5. Finally, Section 6 is dedicated to the conclusions.

2. MEAN STRESS EFFECT ON FATIGUE LIFE: A BRIEF REVIEW

Engineering components and structures are often subjected to cyclic loading with mean stress/mean strain, depending on the testing controlled variable.

As is well-known, the mean stress has a significant influence on the fatigue life **[23]**. As a matter of fact, a tensile mean stress/strain has a detrimental effect on metal fatigue strength, due to the fact that such a stress/strain, by holding the crack faces open, facilitates the growth process and, hence, strongly reduces fatigue life **[24-26]**. Conversely, a compressive mean normal stress/strain has a beneficial effect on fatigue strength, since such a stress/strain, holding closed the crack faces, causes crack growth retardation, and enhances the fatigue lifetime **[27]**.

Under LCF regime, the material response is different, depending on the testing controlled variable. Under strain-controlled uniaxial fatigue tests with mean normal strain (**Figure 2(a)**), mean stress relaxation is observed (**Figure 2(b)**) being characterised by a quick decrease of the mean stress value in the early stage of fatigue life, until a stable condition (named steady state condition) is attained.

The pioneering work by Ellyin **[28]**, who observed such a phenomenon, deserves to be mentioned. More precisely, Ellyin performed uniaxial fatigue tests on a carbon low alloy steel, noticing that the occurrence of plastic deformation resulted in a mean normal stress which fully or partially relaxed during the loading cycles (**Figure 2(b)**).

Figure 2.

According to Ellyin's experimental outcomes **[28]**, the mean stress dropped to 30% of its initial value after one hundred loading cycles, and then tended to a steady state condition at about one thousand cycles, when the mean stress reached about 10% of its initial value. Moreover, Ellyin also observed that the rate of the mean stress relaxation was greater for higher values of the mean strain. As a matter of fact, according to Lee et al. **[29]**, the rate and the amount of relaxation and the stable value of the mean stress are dependent on loading conditions, structural component geometry and material.

In such a context, different relationships are available in the literature in order to take into account the effect of mean stress relaxation on specimen fatigue lifetime, the specimen being under strain-controlled uniaxial fatigue test. For example, they are those by Smith **[30]**, Morrow **[31]**, Smith-Watson-Topper (SWT) **[13]**, Walker **[32]**, and Manson-Halford **[33]**.

According to the published literature **[34]**, the most popular relationship is the SWT one, since it provides accurate estimations in terms of fatigue life for a wide range of metals. More precisely, Smith and co-workers proposed, for uniaxial loading, a fatigue damage parameter equal to the product of the applied normal strain amplitude ε_a and the maximum normal stress $\sigma_{\max}$ **[13]**. Such a parameter was implemented in the well-known

tensile Manson-Coffin equation, obtaining the SWT relationship to compute the number N_f of loading cycles to failure:

$$\sigma_{\max} \cdot \varepsilon_a = \left[\frac{(\sigma'_f)^2}{E} (2N_f)^{2b} + \sigma'_f \, \varepsilon'_f \, (2N_f)^{b+c} \right] \quad (1)$$

where E is the Young modulus, and σ'_f, ε'_f, b, c are material constants which can be determined by running appropriate experimental uniaxial fatigue tests.

It is worth noting that the SWT relationship was developed considering only the effect of the mean value of the axial stress and neglecting that of the applied mean strain. As a matter of fact, it was experimentally observed that the applied mean strain does not contribute to the crack opening mechanisms when the mean stress relaxation tends to a steady state condition **[28]**.

In order to take into account the mean stress effect in presence of multiaxial fatigue loading, the SWT relationship can be implemented in different multiaxial fatigue criteria and, in particular, in those based on the critical plane approach **[35-37]**. The most popular implementation was developed by Socie **[3,38]**, taking into account the maximum value of the normal stress and the amplitude of the normal strain at the verification point into Eq.(1), considering the plane which experiences the maximum value of the principal strain range.

By following a strategy similar to that adopted by Socie **[38]**, the present paper is dedicated to implement a like SWT relationship **[13]** in the multiaxial critical plane-based criterion

by Carpinteri et al., formulated in terms of strains **[12]**, as is detailed in next Section.

3. STRAIN-BASED CRITERION FORMULATION INCLUDING MEAN STRESS EFFECT

For smooth structural components, fatigue analysis is performed at a material point P (also named verification point) located, in general, on the component surface (**Figure 3(a)**). When the component is subjected to biaxial fatigue loading in strain control, consisting in synchronous constant-amplitude cyclic tension and torsion:

$$\varepsilon_z(t) = \varepsilon_{z,a} \sin\left(\frac{2\pi t}{T}\right) + \varepsilon_{z,m} \tag{2a}$$

$$\gamma_{zt}(t) = \gamma_{zt,a} \sin\left(\frac{2\pi t}{T}\right) + \gamma_{zt,m} \tag{2b}$$

the strain tensor at point P, with respect to the fixed frame $Prtz$ given in **Figure 3(a)**, is represented by:

$$\boldsymbol{\varepsilon}(t) = \begin{bmatrix} -\nu_{eff}\,\varepsilon_z(t) & 0 & 0 \\ 0 & -\nu_{eff}\,\varepsilon_z(t) & \frac{1}{2}\gamma_{zt}(t) \\ 0 & \frac{1}{2}\gamma_{zt}(t) & \varepsilon_z(t) \end{bmatrix} \tag{3}$$

where ν_{eff} is the effective Poisson ratio. Note that, since the material has generally a plastic behaviour in LCF regime, the

parameter ν_{eff} has to be taken into account when defining the above strain tensor. An interesting review on the different methods for determining such a parameter is reported in Ref **[39]**.

Figure 3.

According to the strain-based formulation employed in the Carpinteri et al. criterion **[12]**, the critical plane (i.e. the plane considered in fatigue assessment) has to be determined firstly. Note that the present procedure for critical plane determination follows the same philosophy used in the stress-based Carpinteri et al. criterion, formulated for HCF regime **[40]**.

At a generic time instant t, the principal strains $\varepsilon_1, \varepsilon_2$ and ε_3 ($\varepsilon_1 \geq \varepsilon_2 \geq \varepsilon_3$) at point P can be computed from the strain tensor $\boldsymbol{\varepsilon}$ (Eq.(3)), and the corresponding principal strain directions $1, 2, 3$ can be identified by exploiting the principal Euler angles ϕ, θ, ψ. Since the directions of the principal strain axes can change under non-proportional loading, the time varying frame $P123$ corresponding to the time instant when ε_1 attains its maximum value over a loading cycle is assumed to be the averaged principal strain frame $P\hat{1}\hat{2}\hat{3}$.

The orientation of the critical plane, identified by its normal $\mathbf{w}$, is here assumed to form an angle equal to $45°$ with respect to the above direction $\hat{1}$, being the rotation of the $\hat{1}$-axis around the $\hat{2}$ direction and clockwise towards $\mathbf{w}$. The underlying physical

reasoning is to assume that the mechanism of crack growth under LCF is in Stage I, as is stated in Section 1.

Then, we consider a local frame $Puvw$ attached to the critical plane, where the u-axis is defined as the intersection line between the critical plane and the plane containing the $\mathbf{w}$ vector and z-axis, and v-axis forms a right-handed frame together with the u-axis and the z-axis (**Figure 3(b)**).

The displacement vector $\boldsymbol{\eta}$ at point P, related to the critical plane, can be computed from the strain tensor expressed with respect to $Puvw$. Such a vector may be decomposed in:

(i) a normal vector, $\boldsymbol{\eta}_N$:

$$\boldsymbol{\eta}_N(t) = \varepsilon_w(t)\mathbf{w} \tag{4}$$

whose direction is fixed with respect to time. Therefore, its amplitude $\eta_{N,a}$ is given by:

$$\boldsymbol{\eta}_{N,a} = \max_{0\le t<T}\left\|\boldsymbol{\eta}_N(t)\right\| - \min_{0\le t<T}\left\|\boldsymbol{\eta}_N(t)\right\| \tag{5}$$

and

(ii) a tangential vector, $\boldsymbol{\eta}_C$:

$$\boldsymbol{\eta}_C(t) = \frac{1}{2}\gamma_{uw}(t)\mathbf{u} + \frac{1}{2}\gamma_{vw}(t)\mathbf{v} \tag{6}$$

Note that, the tip of $\boldsymbol{\eta}_C$ describes, during the period T, a closed curve Σ on the critical plane. Consequently, the definition of the tangential vector amplitude $\eta_{C,a}$ is not trivial.

In the present paper, the value of $\eta_{C,a}$ is computed by applying the Minimum Bounding Circle Method by Papadopoulos **[19]**. Firstly, such a method involves the determination of the centre of the minimum circumscribed circle to the above curve Σ, by means of the following equation:

$$\boldsymbol{\eta}_{C,m} = \min_{\boldsymbol{\eta}'} \left\{ \max_{0 \le t < T} \left\| \boldsymbol{\eta}_C(t) - \boldsymbol{\eta}' \right\| \right\} \tag{7}$$

where $\boldsymbol{\eta}'$ is a vector on the critical plane, identifying an arbitrary centre. Once $\boldsymbol{\eta}_{C,m}$ is found, the amplitude $\eta_{C,a}$ is obtained as follows:

$$\eta_{C,a} = \max_{0 \le t < T} \left\| \boldsymbol{\eta}_C(t) - \boldsymbol{\eta}_{C,m} \right\| \tag{8}$$

Then in order to reduce the multiaxial strain state to an equivalent uniaxial one, an equivalent strain amplitude $\varepsilon_{eq,a}$ connected to the critical plane is computed as follows:

$$\varepsilon_{eq,a} = \sqrt{\eta_{N,a}^2 + 3\eta_{C,a}^2} \tag{9}$$

Note that, in the original formulation of the criterion **[12]**, the fatigue life assessment was performed by employing such an equivalent strain (Eq.(9)) together with the tensile Manson-Coffin equation:

$$\varepsilon_{eq,a} = \left[\frac{\sigma'_f}{E} \left(2N_f \right)^b + \varepsilon'_f \left(2N_f \right)^c \right] \tag{10}$$

and the fatigue life was determined.

In the present paper, instead, the fatigue life is determined by implementing a like SWT relationship (see Eq.(1)) in the criterion, in order to include the mean stress effect. In particular, the number N_f of loading cycles to failure is obtained from the solution of the following equation:

$$\varepsilon_{eq,a} = \frac{1}{\sigma_{eq,\max}} \left[\frac{\left(\sigma'_f\right)^2}{E} \left(2N_f\right)^{2b} + \sigma'_f \, \varepsilon'_f \, \left(2N_f\right)^{b+c} \right] \tag{11}$$

It is worth noting that the maximum value of the measured axial stress $\sigma_{\max}$ in Eq.(1) is here replaced with the maximum value of an equivalent normal stress σ_{eq} acting on the critical plane. In particular, the maximum value $\sigma_{eq,\max}$ of such an equivalent stress is given by:

$$\sigma_{eq,a} = \sqrt{N_{\max}^2 + \left(\frac{\sigma_{af,-1}}{\tau_{af,-1}} \right)^2 C_a^2} \tag{12}$$

being $N_{\max}$ and C_a the maximum normal stress and the shear stress amplitude related to the critical plane, respectively. Further, $\sigma_{af,-1}$ is the fully-reversed normal stress fatigue strength, and $\tau_{af,-1}$ is the fully-reversed shear stress fatigue strength. Note that Eq.(12) is equal to that implemented in the critical plane-based criterion proposed by Carpinteri et al. in terms of stresses **[40]**. For the sake of simplicity, the fatigue limit ratio $\sigma_{af,-1}/\tau_{af,-1}$ is

herein assumed to be equal to $\sqrt{3}$ (typical value of ductile metals, at the hard/mild border) and, consequently, Eq.(12) turns out to be:

$$\sigma_{eq,a} = \sqrt{N_{\max}^2 + 3C_a^2} \tag{13}$$

We should point out that the present formulation of the Carpinteri et al. criterion can be applied even in the case of pure torsional loadings, whereas the original SWT strain-life curve (Eq.(1)) cannot be used for torsion fatigue data since $\sigma_{\max}$ turns out to be equal to 0.

4. FATIGUE TESTS ON INCONEL 718 ALLOY

In order to check the accuracy of the novel formulation presented in Section 3, some experimental data are selected from the literature **[20-22]**. In particular, the specimens here examined are made of Inconel 718 alloy, with the following mechanical properties: elastic modulus $E = 208500 MPa$, yield strength $\sigma_{y\,0.2\%} = 1160 MPa$, ultimate tensile strength $\sigma_u = 1420 MPa$, and torsional modulus $G = 77800 MPa$. The fatigue properties of such an alloy are listed in Table 1. The effective Poisson ratio ν_{eff} is assumed to be equal to 0.5.

Table 1.

Seventeen loading conditions, grouped in eight test series, are analysed and, as is shown in **Table 2**, they are characterised by both zero and non-zero mean values.

Table 2.

The uniaxial fatigue tests under tension and torsion loading were performed on solid smooth specimens with diameter of $6.3mm$ and gage length of $25mm$. Nominal strain amplitudes applied to such specimens are listed in **Table 2** (see tests from No. T1 to No. T6).

The biaxial fatigue tests under combined tension and torsion loading were performed on thin-walled tubular specimens with internal diameter of $25mm$, wall thickness of $2mm$, and gage length of $25mm$. Nominal strain amplitudes applied to such specimens are listed in **Table 2** (see tests from No. T7 to No. T17).

All tests were conducted by using an MTS Model 809 axial-torsion test system, in strain-control in the LCF regime. Axial displacements were measured by a linear variable differential transducer, and rotations by a rotary variable differential transducer.

Stress-strain loop data were registered. All uniaxial tests and biaxial tests characterised by strain mean values equal to zero showed a strain softening phenomenon (i.e. the uncontrolled

stress decreased with the increasing number of cycles until a stable state was achieved), whereas biaxial tests characterised by strain mean values different from zero showed mean stress relaxation.

The values of measured stress amplitude $\sigma_{z,a}$ and mean stress $\sigma_{z,m}$ are listed in **Table 2**. They were measured for a number of loading cycles related to half fatigue life of each specimen, corresponding to the steady state condition for the mean stress.

During testing, crack growth was monitored by using a replicating technique, where an acetyl cellulose film was periodically melted on the specimen surface, and the resulting replica of the specimen surface topography represented by a cracked and hardened film was removed from the specimen during testing in order to examine it through an optical microscope.

Fatigue crack nucleation and early crack growth were observed to occur on or near planes of maximum shear strain amplitude in each specimen.

The specimen life N_{exp} corresponding to $1mm$ of crack length was determined through the above replicating technique, where such a life was referred to the crack leading to failure (see **Table 2**).

5. RESULTS AND DISCUSSION

The novel formulation is employed for fatigue life assessment of Inconel 718 alloy specimens, whose experimental campaign **[20-22]** is discussed in Section 4.

In **Figure 4(a)**, a comparison in terms of fatigue life between experimental data, N_{exp}, and theoretical estimation, N_f (Eq.(11)), is shown. The solid line indicates $N_{exp} = N_f$, the dashed lines correspond to N_{exp}/N_f equal to 0.5 and 2 (scatter band 2x), and the dot-dashed lines correspond to N_{exp}/N_f equal to $1/3$ and 3 (scatter band 3x). **Figure 4(a)** shows that 65% and 76% of the estimated results fall within scatter band 2x and 3x, respectively. The values of N_f are also listed in **Table 2**.

Figure 4.

The theoretical results obtained by applying the original formulation of the criterion **[12]** (see Eq.(10)) are plotted in **Figure 4(b)** proving that 53% of the estimated results fall within scatter band 2x, whereas 76% fall within scatter band 3x.

From the comparison between the results reported in **Figure 4**, we can remark that the theoretical results related to the novel formulation are more conservative than the results obtained by applying the original criterion **[12]**. As a matter of fact, the percentage of conservative results is equal to 71% by employing the novel formulation, whereas such a percentage is equal to 53% when the original criterion is applied.

Further considerations on the effectiveness of the present formulation in estimating the fatigue life can be also made by examining the values of the mean square error T_{RMS} computed as follows **[41]**:

$$T_{RMS} = 10^{E_{RMS}} \tag{14}$$

being E_{RMS} given by:

$$E_{RMS} = \sqrt{\frac{\sum_{i=1}^{j} \log^2 \left(N_{exp} / N_f \right)_i}{j}} \tag{15}$$

where j is the number of fatigue data being examined. Note that, if all the computed results fell for instance within the scatter band 3x, the value of T_{RMS} would be lower than 3.

Figure 5 shows the mean square error T_{RMS} determined for the different loading conditions here examined (**Table (2)**), in accordance with both the novel formulation and the original criterion.

Figure 5

The analysis of the results in terms of the mean square error clearly indicates that:

(i) for all fatigue tests (Group No. G1-G8), similar accuracy is obtained by using the novel formulation and the original criterion;

(ii) for uniaxial fatigue tests (Group No. G1-G2), higher accuracy is gained by applying the original criterion, since all the results are within scatter band 3x;

(iii) for all biaxial fatigue tests (Group No. G3-G8), the most accurate result is obtained by employing the novel formulation, with a decrease of the T_{RMS} value up to 17% with respect to that deduced through the original criterion;

(iv) for biaxial fatigue tests characterized by strain mean values different from zero (Group No. G6-G8), higher accuracy is gained by means of the present formulation. Note that, by implementing Eq.(11) in the Carpinteri et al. criterion, the value of T_{RMS} significantly decreases (up to 54%) in comparison with that obtained from the original formulation of such a criterion (see Eq. (10)).

On the basis of such encouraging results, it is worth remarking that the novel formulation provides more accurate results than the original one in the case of mean stress relaxation. Consequently, the implementation of a like SWT relationship in the Carpinteri et al. criterion seems to be a promising tool to assess the fatigue life of metallic structural components under LCF regime and strain control, in presence of loading characterised by both zero and non-zero mean values.

6. CONCLUSIONS

In the present paper, fatigue tests related to Inconel 718 specimens have been analysed by using the critical plane-based multiaxial fatigue criterion by Carpinteri et al., formulated in terms of strain, in conjunction with a model similar to that by Smith-Watson-Topper (SWT). More precisely, both smooth solid specimens and thin-walled tubular specimens subjected to proportional and non-proportional loading consisting of tension, torsion, and combined tension and torsion loading under strain control have been analysed, such loadings being characterised by both zero and non-zero mean values.

The present formulation allows us to analytically estimate the fatigue life of metallic structural components by means of an equivalent normal strain amplitude connected to the critical plane, together with a SWT type of relationship, in order to take into account the mean stress effect on fatigue life. In particular, fatigue life has been analytically computed through the novel formulation and compared with the experimental one, in terms of the number of loading cycles needed to form a surface crack whose length is equal to 1 mm.

The agreement between the experimental data and theoretical fatigue lives is satisfactory and, consequently, the present criterion seems to be able to quite correctly estimate the fatigue

life of a structural component under multiaxial loading (with zero and non-zero mean stress).

Acknowledgements

The authors gratefully acknowledge the financial support of the Italian Ministry of Education, University and Research (MIUR), Research Grant PRIN 2017 No. 2017HFPKZY on "Modelling of constitutive laws for traditional and innovative building materials".

REFERENCES

[1] Suresh S. Fatigue of Materials. 2nd ed. Cambridge University Press; 1998.

[2] Forsyth PJE, A two stage process of fatigue crack growth. Proceedings of Crack Propagation Symposium, Cranfield, Vol. 1. 1961;76-94.

[3] Karolczuk A, Macha E, A review of critical plane orientations in multiaxial fatigue failure criteria of metallic materials, Journal of Fracture 2005; 134: 267–304.

[4] Brown MW, A Crack Propagation Based Effective Strain Criterion, in Biaxial and Multiaxial Fatigue, EGF 3 (Edited by Brown MW and Miller KJ), 1989, Mechanical Engineering Publications, London, pp. 499-510.

[5] Miller KJ, Fatigue under complex stress. Metal Science 1977;11:432-8. https://doi.org/10.1179/msc.1977.11.8-9.432.

[6] Brown MW, Miller KJ, Initiation and growth of cracks in biaxial fatigue. Fatigue Fract Eng Mater. 1979;1:231-46. https://doi.org/10.1111/j.1460-2695.1979.tb00380.x.

[7] Marciniak Z, Rozumek D, Professor Ewald Macha's contribution to the development of methods for multiaxial fatigue life estimation. Int J Fatigue 2016;92:384-94. https://doi.org/10.1016/j.ijfatigue.2016.05.008.

[8] Lu C, Melendez J, Martínez-Esnaola JM, Modelling multiaxial fatigue with a new combination of critical plane definition and energy-based criterion. Int J Fatigue 2017;108:109-15. https://doi.org/10.1016/j.ijfatigue.2017.12.004.

[9] Springer M, Pettermann HE, Fatigue life predictions of metal structures based on a low-cycle, multiaxial fatigue damage model. Int J Fatigue 2018;116:355-65. https://doi.org/10.1016/j.ijfatigue.2018.06.031.

[10] Dowling N, Mean Stress Effects in Stress-Life and Strain-Life Fatigue. SAE Technical Papers 2004. https://doi.org/10.4271/2004-01-2227.

[11] Ince A, Glinka G, A modification of Morrow and Smith-Watson-Topper mean stress correction models. Fatigue Fract Eng Mater. 2011;34:854-67. https://doi.org/10.1111/j.1460-2695.2011.01577.x.

[12] Carpinteri A, Ronchei C, Spagnoli A, Vantadori S, Lifetime estimation in the low/medium-cycle regime using the Carpinteri–Spagnoli multiaxial fatigue criterion. Theor Appl Fract Mech 2014;73:120–7. https://doi.org/10.1016/j.tafmec.2014.06.002.

[13] Smith RN, Watson P, Topper TH, A stress-strain parameter for the fatigue of metals. J Mater 1970;5:767-78.

[14] Gough HJ, Pollard HV, Clenshaw WJ, Some Experiments on the Resistance of Metals to Fatigue under Combined Stresses, Ministry of Supply, Aeronautical Research Council Reports and Memoranda, London, His Majesty's Stationary Office, 1951.

[15] Carpinteri A., Spagnoli A., Multiaxial high-cycle fatigue criterion for hard metals, International Journal of Fatigue 2001; 23: 135-145

[16] Fukuda T., Nisitani H., The background of fatigue limit ratio of torsional fatigue to rotating bending fatigue in isotropic materials and materials with clear-banded structure. In: Biaxial/Multiaxial Fatigue and Fracture, edited by Andrea Carpinteri, Manuel de Freitas, Andrea Spagnoli, European Structural Integrity Society 2003; 31: 285-302.

[17] Sonsino C.M., Influence of material's ductility and local deformation mode on multiaxial fatigue response, Journal of Fatigue 2011; 33: 930-947.

[18] Chaves V., Navarro A., Madrigal C., Vallellano C., Calculating crack initiation directions for in-phase biaxial fatigue loading, International Journal of Fatigue 2014; 58: 166-171.

[19] Papadopoulos IV, Davoli P, Gorla C, Filippini M, Bernasconi A, A comparative study of multiaxial high-cycle fatigue criteria for metals. International Journal of Fatigue 1997; 19: 219–235.

[20] Socie DF, Shield TW, Mean Stress Effects in Biaxial Fatigue of Inconel 718. J Eng Mater 1984;106:227-32. https://doi.org/10.1115/1.3225707.

[21] Socie D, Waill L, Dittmer D, Biaxial Fatigue of Inconel 718 Including Mean Stress Effects. ASTM Special Technical Publication STP 853 1985;463-81.

[22] Socie D.F., Kurath P., Koch J.L., A Multiaxial Fatigue Damage Parameter. Proceedings of the 3rd International Conference on Multiaxial Fatigue and Fracture 2013;535-50.

[23] Stephens RI, Fatemi A, Stephens AA, Fuchs HO. Metal Fatigue in Engineering. New York: John Wiley; 2001.

[24] Xia Z, Kujawski D, Ellyin F, Effect of mean stress and ratcheting strain on fatigue life of steel. Int J Fatigue 1996;18:335-341. https://doi.org/10.1016/0142-1123(96)00088-6.

[25] Ellyin F. Fatigue damage, crack growth and life prediction. London: Chapman & Hall; 1997.

[26] Papadopoulos IV, A new criterion of fatigue strength for out-of-phase bending and torsion of hard metals. Int J Fatigue 1994;16:377–84. https://doi.org/10.1016/0142-1123(94)90449-9.

[27] Gough HJ, Pollard HV, The strength of metals under combined alternating stresses. Proc Instn Mech Engrs 1953;131:3-54.

[28] Ellyin F, Effect of tensile-mean-strain on plastic strain energy and cyclic response. J Eng Mater Technol 1985;107:119–125. https://doi.org/10.1115/1.3225786.

[29] Lee C-H, Do VNV, Chang K-H, Analysis of uniaxial ratcheting behavior and cyclic mean stress relaxation of a duplex stainless steel. Int J Plasticity 2014;62:17-33. https://doi.org/10.1016/j.ijplas.2014.06.008.

[30] Smith JO, The Effect of Range of Stress on the Fatigue Strength of Metals. Bulletin No. 334, University of Illinois, Engineering Experiment Station, Urbana, 1942.

[31] Morrow J. Fatigue Properties of Metals. In: Graham JA, Mllan JF, Appl FJ, editors. Fatigue Design Handbook, Warrendale: SAE; 1968, p. 21-9.

[32] Walker K. The effect of stress ratio during crack propagation and fatigue for 2024-T3 and 7075-T6 aluminum. In: Effects of Environment and Complex Load History on Fatigue Life, ASTM STP 462. American Society for Testing and Materials, West Conshohocken; 1970 p. 1–14.

[33] Manson SS, Halford GR, Practical implementation of the double linear damage rule and damage curve approach for treating cumulative fatigue damage. Int J Fract 1981;17:169–72. https://doi.org/10.1007/BF00053519.

[34] Dowling NE. Mechanical behaviour of materials. Upper Saddle River: Prentice-Hall; 1999.

[35] Chen X, Xu S-Y, Huang D-X, Critical plane-strain energy density criterion of multiaxial low-cycle fatigue life. Fatigue Fract Eng Mater Struct 1999;22:679–86. https://doi.org/10.1046/j.1460-2695.1999.00199.x.

[36] Gates NR, Fatemi A, On the consideration of normal and shear stress interaction in multiaxial fatigue damage analysis. International J Fatigue 2017;100:322-36. https://doi.org/10.1016/j.ijfatigue.2017.03.042.

[37] Yu ZY, Zhu SP, Liu Q, Liu Y, A New Energy-Critical Plane Damage Parameter for Multiaxial Fatigue Life Prediction of Turbine Blades. Materials 2017;10:513. https://doi.org/10.3390/ma10050513.

[38] Socie DF, Multiaxial fatigue damage models. J Eng Mater 1987;109:292–8. https://doi.org/10.1115/1.3225980.

[39] Carpinteri A, Ronchei C, Scorza D, Vantadori S, Fatigue life estimation for multiaxial low-cycle fatigue regime: the influence of the effective Poisson ratio value. Theor Appl Fract Mech 2015;79: 77-83. https://doi.org/10.1016/j.tafmec.2015.06.013.

[40] Carpinteri A, Spagnoli A, Vantadori S, Multiaxial fatigue assessment using a simplified critical plane-based criterion, Int J Fatigue 2011;33:969–76.https://doi.org/10.1016/j.ijfatigue.2011.01.004.

[41] Łagoda T, Walat K, Lifetime of semi-ductile materials through the critical plane approach. Int J Fatigue 2014;67:73-7. https://doi.org/10.1016/j.ijfatigue.2013.11.019.

Submitted to International Journal of Fatigue –
Virtual Special Issue: Multiaxial Fatigue 2019
October 2019
REVISED Version R1, November 2019

MEAN STRESS EFFECT ON FATIGUE LIFE ESTIMATION FOR INCONEL 718 ALLOY

Sabrina Vantadori*, Andrea Carpinteri*, Raimondo Luciano**,
Camilla Ronchei***, Daniela Scorza**, Andrea Zanichelli*

*Department of Engineering & Architecture, University of Parma,
Parco Area delle Scienze 181/A, 43124 Parma, Italy

** Department of Engineering, University of Naples Parthenope,
Centro Direzionale Isola C4, 80143 Naples, Italy

*** Department of Civil Engineering, University of Calabria,
via Pietro Bucci, 87036 Arcavacata di Rende (CS), Italy

Corresponding author: sabrina.vantadori@unipr.it

FIGURES AND TABLES

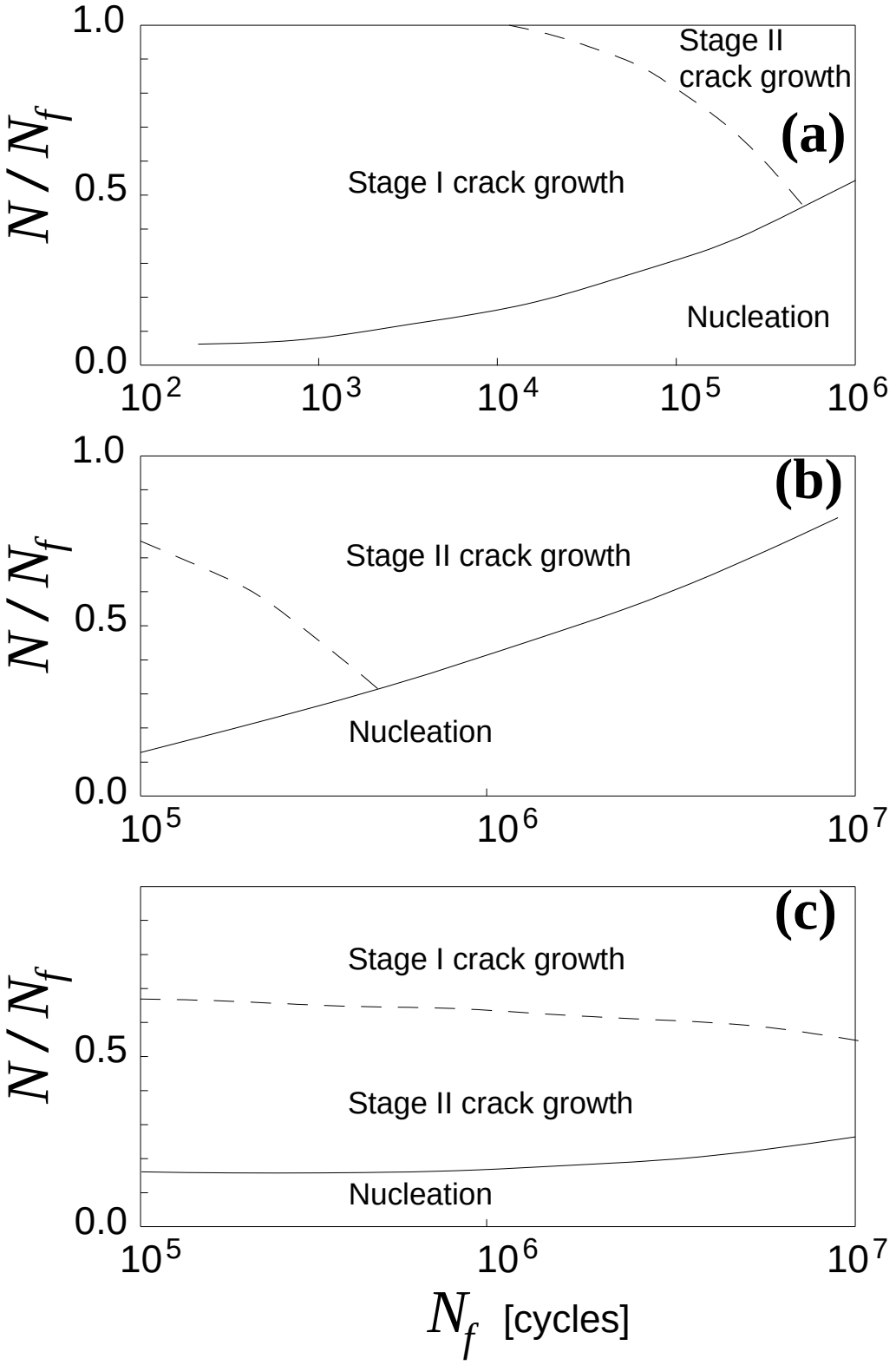

Figure 1. Schematic representation of transition between crack nucleation, Stage I and Stage II crack growth: (a) ductile materials under LCF, (b) extremely brittle materials under HCF, (c) brittle materials under HCF.

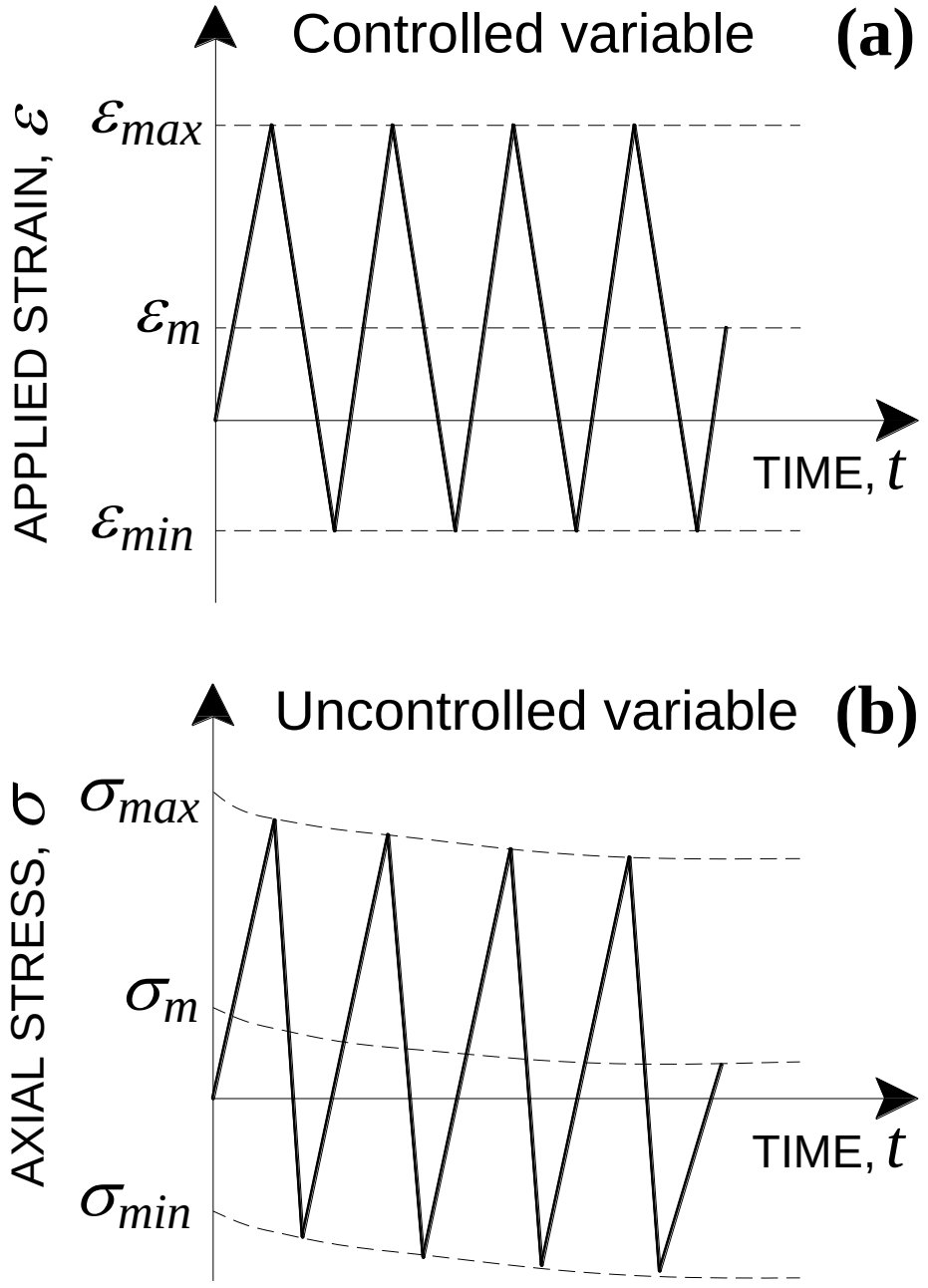

Figure 2. Strain-control uniaxial testing: (a) controlled variable; (b) uncontrolled variable.

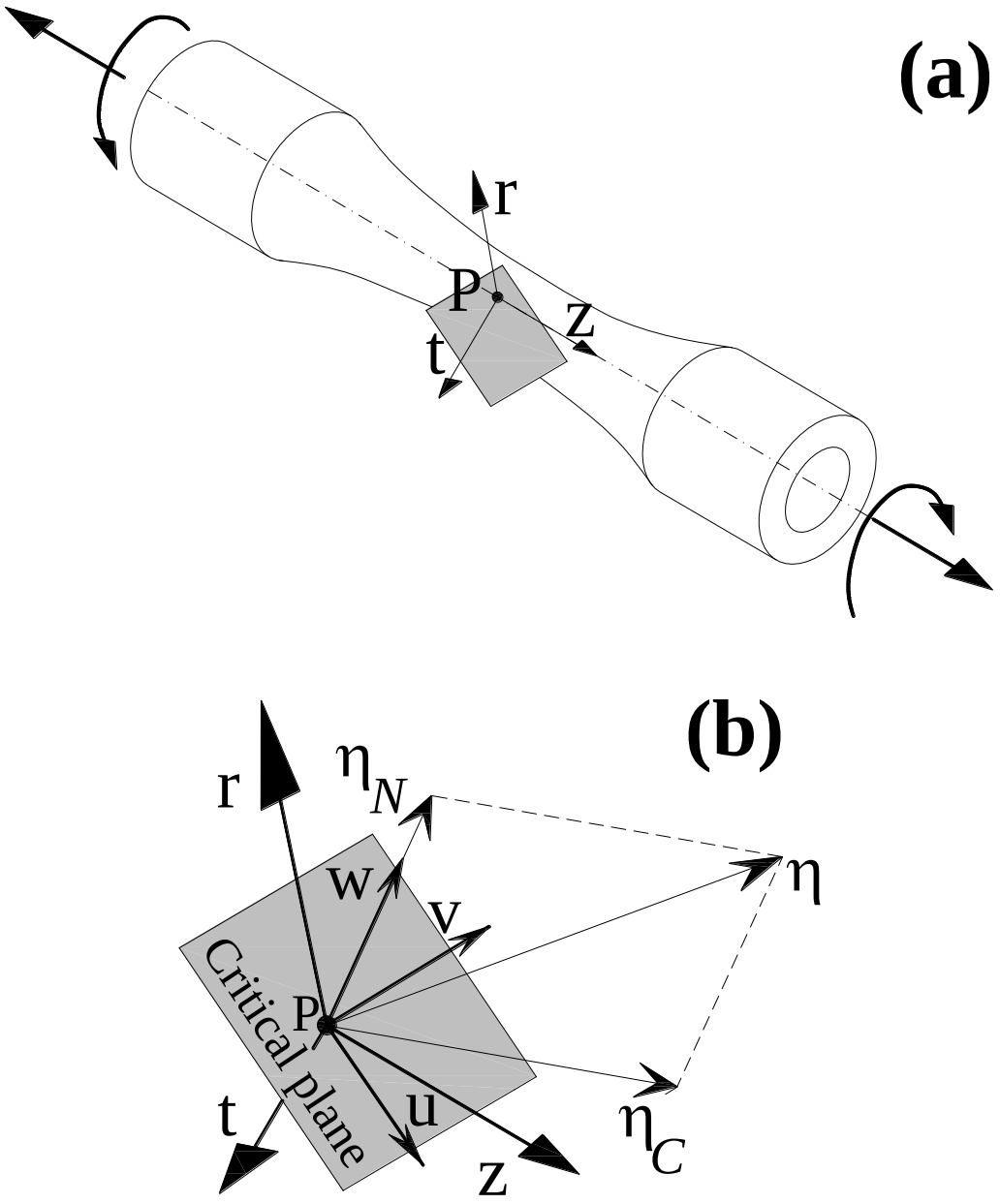

Figure 3. (a) Tested specimen under biaxial fatigue: *Prtz* fixed frame, (b) *Puvw* frame and displacement vector components related to such a frame.

Table 1. Fatigue properties of Inconel 718 alloy examined.

PROPERTY	$\sigma_{af,-1}$ [MPa]	$\tau_{af,-1}$ [MPa]	σ'_f [MPa]	b [-]	ε'_f [-]	c [-]
	442	251	3950	-0.151	1.5	-0.761

Table 2. Loading conditions examined, fatigue lives computed by applying the novel formulation, and experimental fatigue lives.

Group No.	Test No.	$\varepsilon_{z,a}$	$\varepsilon_{z,m}$	$\gamma_{zt,a}$	$\gamma_{zt,m}$	β [°]	$\sigma_{z,a}$ [MPa]	$\sigma_{z,m}$ [MPa]	$\tau_{zt,a}$ [MPa]	$\tau_{zt,m}$ [MPa]	N_{exp} [cycles]	N_f [cycles]
G1	**T1**	0.010	0	0	0	---	1095	-26.5	0	0	1025	585
	T2	0.005	0	0	0	---	927.5	-24.5	0	0	12250	3356
G2	**T3**	0	0	0.0176	0	---	0	0	600.5	2.5	845	441
	T4	0	0	0.0087	0	---	0	0	536.5	-5.5	7100	2498
	T5	0	0	0.0054	0	---	0	0	415	-5	34850	13729
	T6	0	0	0.0043	0	---	0	0	304.5	-29	109500	39950
G3	**T7**	0.0071	0	0.0123	0	0	755	-27.5	431	15.5	1100	962
	T8	0.0035	0	0.0061	0	0	633	-56.5	388	16	7500	7914
	T9	0.0015	0	0.0027	0	0	326	-1	200.5	-5.5	225000	533283
G4	**T10**	0.0035	0	0.0062	0	45	515	-19	495.5	28	5815	8077
G5	**T11**	0.0071	0	0.0123	0	90	999	-30.5	559.5	-3.5	440	3561
	T12	0.0035	0	0.0062	0	90	758	-26.5	463	-5.5	3860	19661
G6	**T13**	0.0035	0	0.0063	0.0063	180	634	90.5	393.5	123	4000	3379
G7	**T14**	0.0071	0.0071	0.0123	0.0123	0	751	119	419	-71	1050	962
	T15	0.0035	0.0035	0.0063	0.0063	0	646	170	396	52	4800	7025
	T16	0.0015	0.0015	0.0026	0.0026	0	311	327	190	198	53000	670977
G8	**T17**	0.0035	-0.0035	0.0063	-0.0063	0	596	-201.5	378	-36	6500	7025

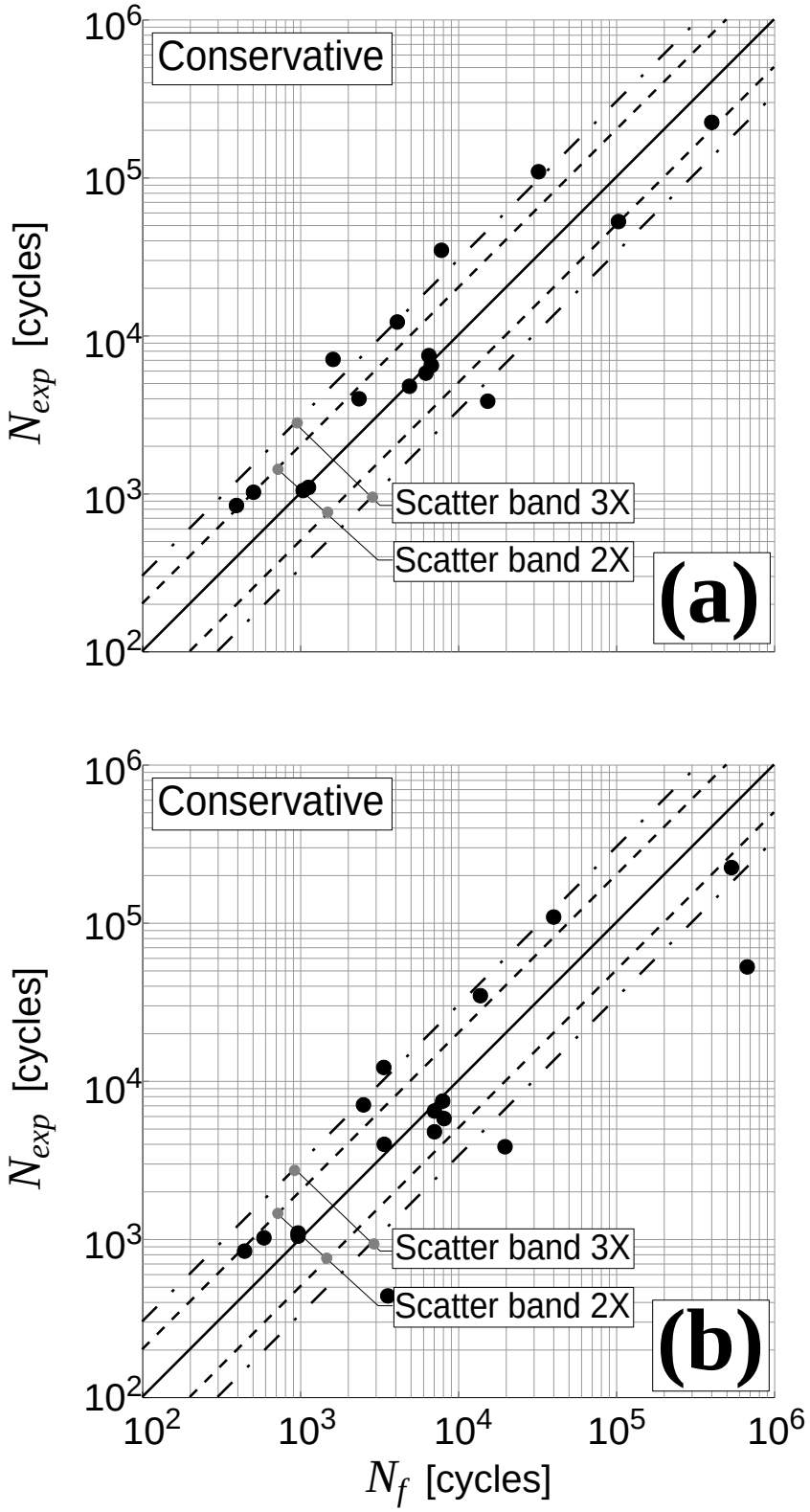

Figure 4. Comparison between theoretical, N_f, and experimental, N_{exp}, fatigue lives by applying: (a) the novel formulation, and (b) the original criterion **[11]**.

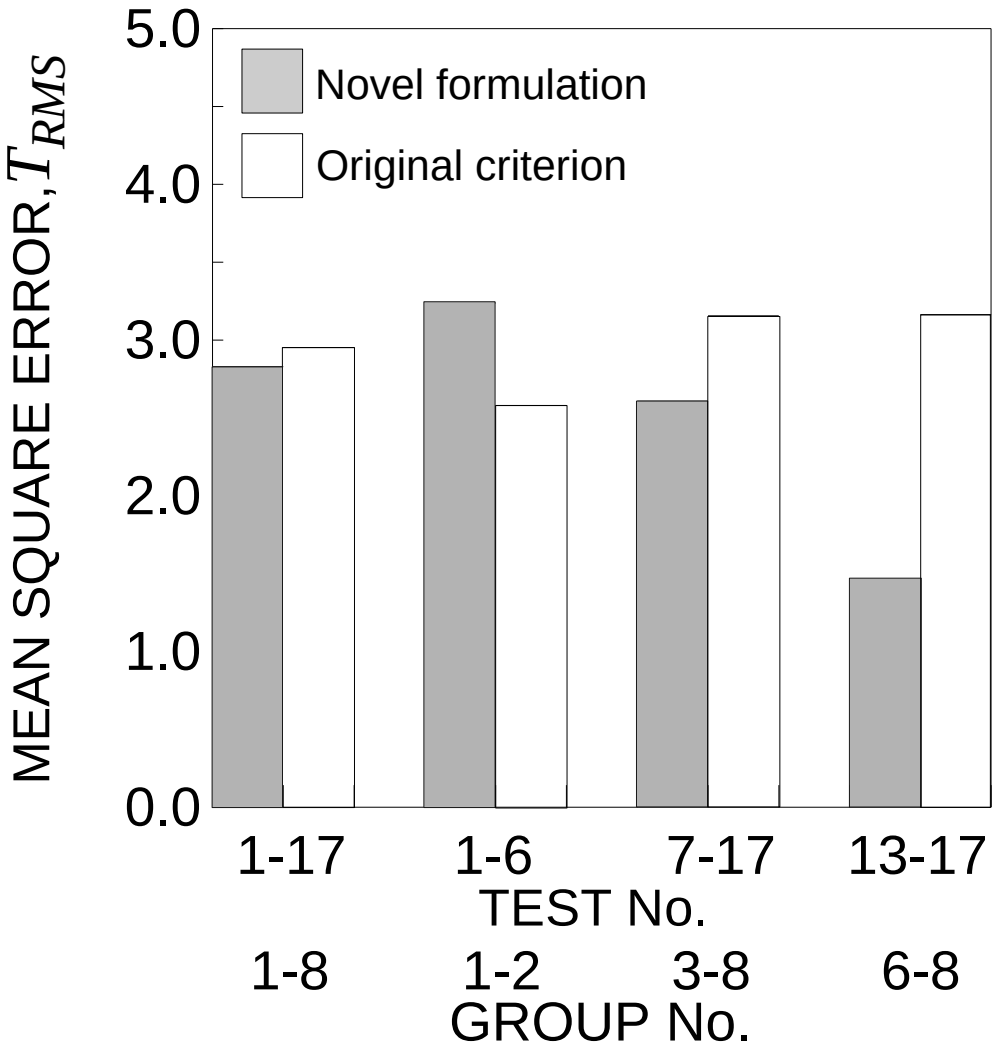

Figure 5. Mean square error determined by applying both the present formulation and the original criterion.